Description and Measurement of Landsat TM Images Using Fractals

Nina Siu-Ngan Lam
Department of Geography and Anthropology, Louisiana State University, Baton Rouge, LA 70803

ABSTRACT: Landsat TM images of three different land types taken from coastal Louisiana were measured using the fractal model. Fractal dimensions of these TM surfaces were found to be generally higher than most real-world terrain surfaces, with resultant values ranging from 2.54 to 2.87 at the scale range between 25 m and 150 m. Among the three land types, the urban area was found to be most spatially complex with high D values occurring in bands 2 and 3. This is followed by the coastal and rural land types which both exhibit high D values in band 1.

INTRODUCTION

IN THE DECADE since Mandelbrot first coined the term "fractals" (Mandelbrot, 1977), studies on fractals have grown explosively. Applications of fractals range from simulation and generation of extra-terrestrial planets and objects in motion pictures and video games (e.g., Mandelbrot, 1983; Batty, 1985) to pure scientific analyses of patterns, forms, and structures. The development of fractals has been so rapid that, in 1986, there were 239 references related to fractals, as compared with only two in 1975 (De Cola, 1987). Indeed, as the physicist John A. Wheeler has said, "no one is considered scientifically literate today who does not know what a Gaussian distribution is, or the meaning and scope of the concept of entropy. It is possible to believe that no one will be considered scientifically literate tomorrow who is not equally familiar with fractals" (Batty, 1985).

In spite of the numerous applications, the use of fractals in remote sensing has not yet been closely examined. The primary objective of this study is to explore whether such a new concept can be applied to remote sensing. If digital remotely sensed data are considered to be one form of spatial surfaces, then the complexity of these spatial surfaces should be apt for description and measurement by a fractal model. The question is how would these remotely sensed data compare with other surfaces, such as digital terrain model surfaces (DTM/DEM), which have been measured by the fractal approach. Additionally, how would different types of remotely sensed surfaces, such as urban or rural land types, behave according to the fractal model. This paper will focus on the fractal measurement and description of Landsat Thematic Mapper (TM) digital surfaces.

A brief review of the basic concepts, applications, and problems of fractals may be helpful. This review section is meant to serve as only a short introduction to those readers who are unfamiliar with fractals. For a more detailed review and discussion on the use of the fractals in the spatial and earth sciences, see Goodchild and Mark (1987).

FRACTALS — A BRIEF REVIEW

In classical geometry (i.e., Euclidean geometry), the dimension of a curve is defined as 1, a plane as 2, and cube as 3. This is called topological dimension (D_t) and is characterized by integer values. In fractal geometry, the dimension D of a curve can be any value between 1 and 2, according to the curve's degree of complexity. Similarly, a plane may have a dimension whose value lies between 2 and 3. This concept of fractional dimension was first formulated by mathematicians Hausdorff and Besicovitch (Mandelbrot, 1977). Mandelbrot (1977) later called it fractal dimension and defined fractals as "a set for which the Hausdorff-Besicovitch dimension strictly exceeds the topological dimension" (p.15). Since then, the definition of fractals has been modified and a complete definition is still lacking (Feder, 1988).

The derivation of fractals arises from the fact that most spatial patterns of nature, including curves and surfaces, are so irregular and fragmented that classical geometry finds it difficult to provide tools for analysis of their forms. For example, the coastline of an island is neither straight nor circular, and no other classical curve can serve in describing and explaining its form without extra artificiality and complexity.

The key concept of fractals is the use of self-similarity to define D. Many curves and surfaces are statistically "self-similar," meaning that each portion can be considered as a reduced-scale image of the whole. Thus, D can be defined as

$$D = \log N / \log(1/r) \tag{1}$$

where $1/r$ is a similarity ratio, and N is the number of steps needed to traverse the curve (Mandelbrot, 1967). Figure 1 illustrates the relationship between the number of steps (N) and the similarity ratio ($1/r$). Practically, the D value of a curve (e.g., coastline) is estimated by measuring the length of the curve using various step sizes. The more irregular the curve, the greater

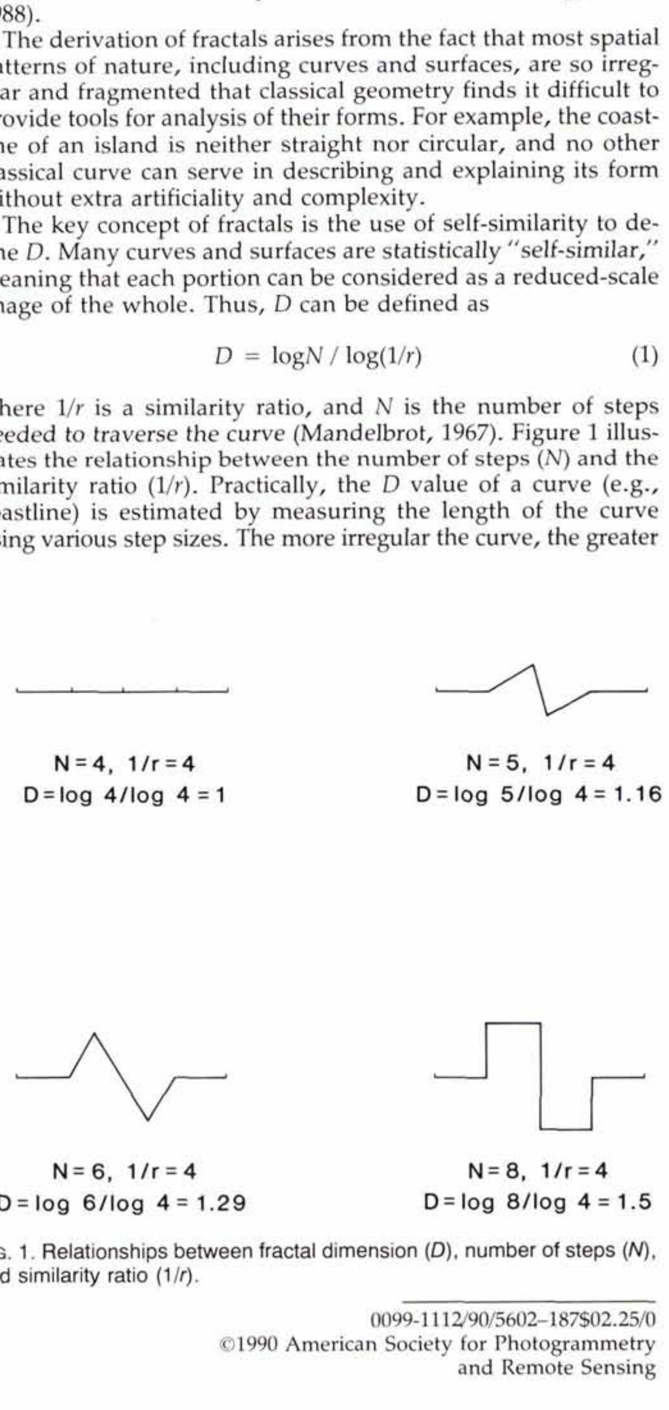

FIG. 1. Relationships between fractal dimension (D), number of steps (N), and similarity ratio ($1/r$).

PHOTOGRAMMETRIC ENGINEERING AND REMOTE SENSING,
Vol. 56, No. 2, February 1990, pp. 187-195.

0099-1112/90/5602-187$02.25/0

increase in length as step size decreases. And D can be estimated by the following regression equation:

$$\text{Log}L = C + B\ \text{log}G \tag{2}$$
$$D = 1 - B \tag{3}$$

where L is the length of the curve, G is the step size, B is the slope of the regression, and C is a constant. This equation is strikingly similar to Richardson's empirical law on coastline length measurement (Richardson, 1961). The D value of a surface can be estimated in a similar fashion and is discussed in detail in the methods section.

Another aspect of fractal concepts is the generation of fractal curves and surfaces. Based on the model of Brownian motion in physics, together with the concept of self-similarity, Mandelbrot (1975) derived a general stochastic model for generating curves and surfaces of various dimensions. Previous research has found that curves and surfaces generated with a D value between 1.1 to 1.3 and 2.1 to 2.3 would look very much like real curves (e.g., coastlines) and surfaces (e.g., topography), respectively. Several approaches can be used to generate fractal curves and surfaces, including the shear displacement method, the modified Markov method, the inverse Fourier transform method, and the recursive subdivision method (e.g., Carpenter, 1981; Dutton, 1981; Fournier *et al.*, 1982; Goodchild, 1980; Mandelbrot, 1983). Figure 2 shows some example surfaces with different D values generated using a shear displacement algorithm written by Goodchild (1980).

Applications of fractals can generaly be classified into two major types. The first set of applications uses fractals as a model to simulate real-world, as well as extra-terrestrial, objects for both analytical and display purposes. Simulation of objects includes coastlines (Carpenter, 1981; Dutton, 1981), terrain, trees, clouds, mountainscapes, natural landscapes (Mandelbrot, 1983; Batty, 1985), cities (Batty and Longley, 1986), particle growth, planet rise, dragon, and other computer graphic applications (Mandelbrot, 1983; Peitgen and Richter, 1986; Peitgen and Saupe, 1988). Fractal surfaces have been used as test data sets to examine the performance of various spatial interpolation methods (Lam, 1982; 1983) and the efficiency of a quadtree data structure (Mark and Lauzon, 1984). Fractal curve generation, on the other hand, has been used as an interpolation method and as the inverse of curve generalization by adding more details to the generalized curve (Carpenter, 1981; Dutton, 1981; Jiang, 1984). These kinds of applications have made the fractal model a very popular tool, largely because of its visual impacts and its ability to generate real-world-like objects.

The second set of applications utilizes the fractal dimension as an index for describing the complexity of curves and surfaces. For example, fractals have been used to examine coastlines (Shelberg *et al.*, 1982), particle shape (Clark, 1986), physical properties of amorphous or glassy materials (Orbach, 1986), rainfall and clouds (Lovejoy and Mandelbrot, 1985), terrain (Mark and Aronson, 1984; Shelberg *et al.*, 1983), shoreline erosion (Philips, 1986), coral reefs (Bradbury and Reichelt, 1983; Mark, 1984), ocean bottom relief (Barenblatt *et al.*, 1984), underside of sea ice (Rothrock and Thorndike, 1980); soils (Burrough, 1983), and the central place theory (Arlinghaus, 1985). In addition, Goodchild (1980), in a pioneer article, demonstrated that fractal dimension can be used to predict the effects of cartographic generalization and spatial sampling, a result which may help in determining the resolution of pixels and polygons used in

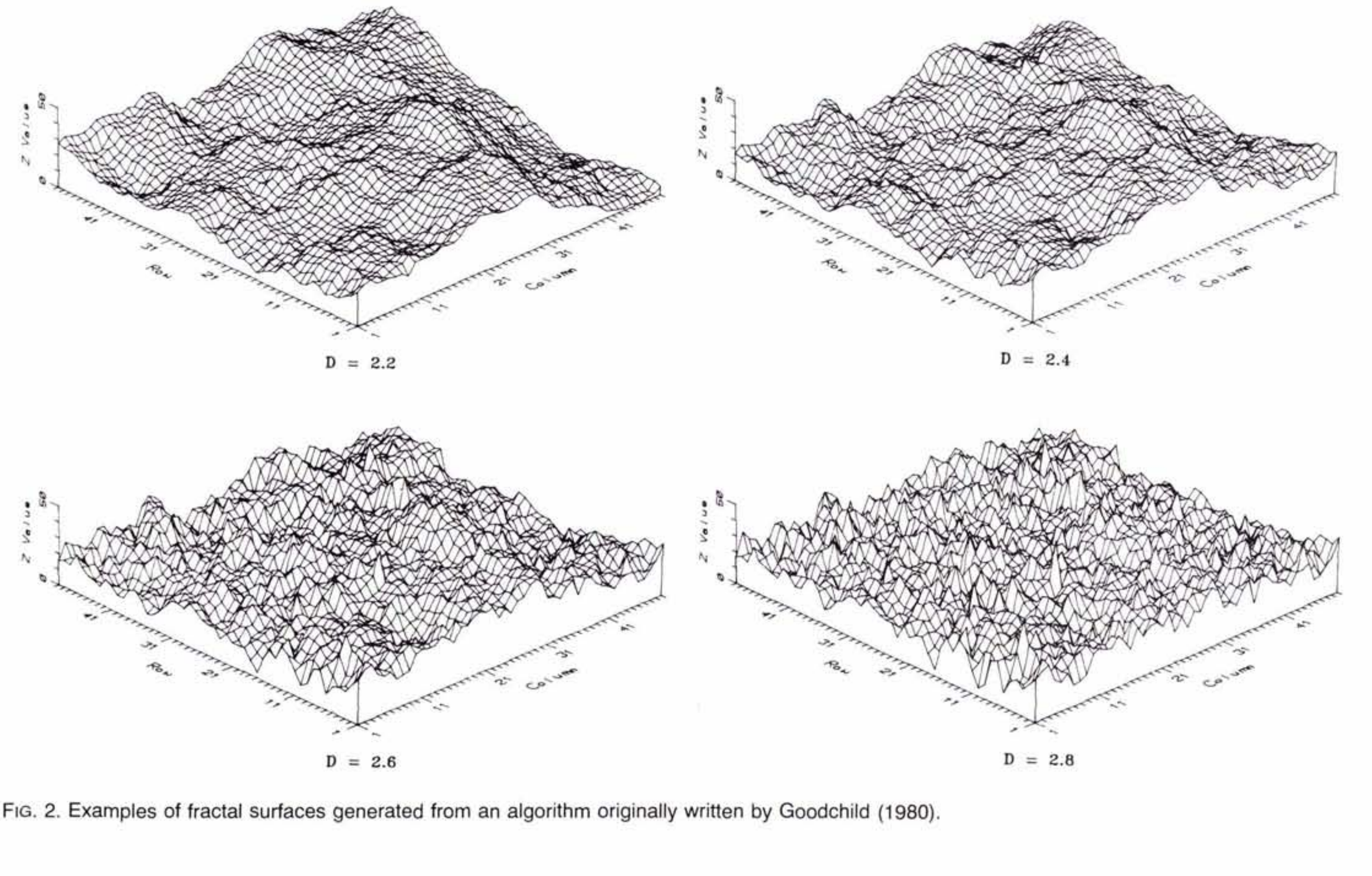

FIG. 2. Examples of fractal surfaces generated from an algorithm originally written by Goodchild (1980).

studies related to geographic information systems and remote sensing.

The fractal model is a fascinating tool for simulating landscapes and objects in the movie industry and for some other computer graphics applications. However, the use of fractals in the spatial and earth sciences, and in remote sensing, could be limited by problems at two levels. At the theoretical level, the self-similarity property underlying the fractal model assumes that the form or pattern of the spatial phenomenon remains unchanged throughout all scales. This further implies that one cannot determine the scale of the spatial phenomenon from its form or pattern. This is considered unacceptable in principle and hence it has been rejected by a number of geoscientists (Hakanson, 1978). Empirical studies have shown that most real-world coastlines and surfaces are not pure fractals with a constant D. Instead, D varies across a range of scales (Goodchild, 1980; Mark and Aronson, 1984). These findings, however, can be interpreted positively. Rather than using D in the strict sense as defined by Mandelbrot (1983), it is possible to use the D parameter to summarize the scale changes of the spatial phenomenon. Consequently, some interpretation of its processes at specific ranges of scales could be made.

Recently, Goodchild and Mark (1987) suggested using fractal surfaces as a null-hypothesis terrain or norm whereby further simulation of various geomorphic processes can be made. Similarly, Loehle (1983), in a paper examining the applications of fractal concepts in ecology, suggested the use of the D parameter to summarize the effect of a certain process up to particular scale. He also proposed the use of the self-similarity property as a null hypothesis. For example, if wind turbulence, a major cause of tree breakage, is a self-similar process, then one can use the property as a null hypothesis to test the forest canopy breakage pattern. Any deviations from the self-similar pattern would mean the possible existence of other factors such as fires or beaver damages. Thus, the application of fractals allows not only a different and convenient way of describing spatial patterns, but also the generation of hypotheses about the causes of the patterns. Although the latter application may be premature at this time, the suggestions made in these studies open another new direction for applying fractals. Clearly, the potential of fractal applications has not yet been fully realized.

The second problem of applying fractals, the technical problem of measuring fractals, is equally intriguing. Several aspects of the problem can be identified. First of all, the fact that self-similarity exists only within certain ranges of scales makes it difficult to identify the breaking point. This affects the final D value, which is then used to characterize the curve or surface. The calculation of fractal dimensionality for surfaces presents an additional technical problem. A recent empirical study has shown that, for the same surface, different D values could result from using different algorithms, with a range of as low as 2.01 to as high as 2.33 (Roy *et al.*, 1987). Finally, all the existing methods have so far been applied only to regular grid data, such as digital terrain model data and, in this paper, Landsat TM data. Fractal measurement of many other socio-economic phenomena, such as population and disease distributions, is another challenge. These data are typically reported in an aggregate polygonal form, with irregular boundaries and possibly holes (in the forms of lakes or islands) or missing data. The existing algorithms will have to be modified and extra steps will have to be taken before the actual measurement takes place.

RESEARCH OBJECTIVES

Despite the theoretical and technical problems, the fractal model seems to have potential for providing new norms and perspectives in the measurement, analysis, and interpretation of digital remotely sensed data. First, fractal dimensions of remotey sensed data, such as TM images, could be calculated and used as a measure of spatial complexity or information content. Different types of remotely sensed data, including data of different land types, sensors, and bands, could be compared and analyzed based on the fractal dimensions. Second, the dimension values could be compared with other spatial complexity measures. Third, if different types of remotely sensed images have unique fractal dimensions, one could base on the dimension values a control to the fractal surface generation algorithms for the simulation of remotely-sensed images.

This study focuses on the first step of fractal analysis using Landsat TM images. In particular, the objectives of this study are (1) to compare the fractal dimensions of the Landsat TM surfaces with those of the DTM surfaces measured in other studies. Given the same spatial resolution, it is expected that TM surfaces are more spatially complex and thus have higher dimension values, because TM images are basically synoptic and contain both topographic as well as non-topographic information. (2) To examine if different land types, presumably of different levels of spatial complexity, would have distinct fractal dimensions. For example, would a typical middle-size city have a unique dimension as compared with a rural area? (3) And finally, to analyze if different bands have different levels of complexity in different types of surfaces. The results from the last two objectives of this study will be useful to the display and analysis as well as future generation of TM images.

DATA

Three study areas were extracted from three different Landsat TM quadrants of coastal Louisiana for this study. These Landsat data were purchased by the Coastal Management Division of the Louisiana Department of Natural Resources. A small subset, approximately 6 kilometres on a side, was selected from each quadrant. The subsets were then rectified, using UTM coordinates, to a 5-km by 5-km area with resulting pixels measuring 25 m by 25 m. Each subset contains a total of 201 by 201 = 40,401 pixels. The selection of these three study areas was primarily based on the availability of the data and the typical land types they represent. The use of a small subset instead of a full TM quadrant is preferred, partly due to the machine size (using PC ERDAS) and processing time, and partly due to the fact that a full TM quadrant often encompasses a wide variety of land types and thus will not be suitable for the present study.

Plate 1a shows the locations of the Landsat TM quadrants and the subsets in the quadrants used in this study. Table 1 lists the image acquisition dates of the Landsat scenes and the UTM coordinates of the three subsets. Plates 1b, 1c, and 1d display the study areas using bands 2 (blue), 3 (green), and 4 (red). Study area A covers part of the City of Lake Charles in southwestern Louisiana. It represents an urban landscape with a city size of about 75,000 people. Study area B covers part of the

TABLE 1. LOCATIONS OF THE THREE STUDY AREAS

Study area (within 7.5 min. quadrangle)	Subset from TM-Quadrant	Image Date	Path/ Row	Upper Left UTM Coordinates (Zone 15)
A. Lake Charles	Calcasieu & White Lakes (Quad. 4)	11-30-84	24/39	478000, 3345000
B. Kemper	Atchafalaya Basin (Quad. 2)	1-26-85	22/40	623306, 3297559
C. Bay Tambour	Timbalia Bay Breton Sound (Quad. 4)	12-2-84	23/39	779918, 3251911

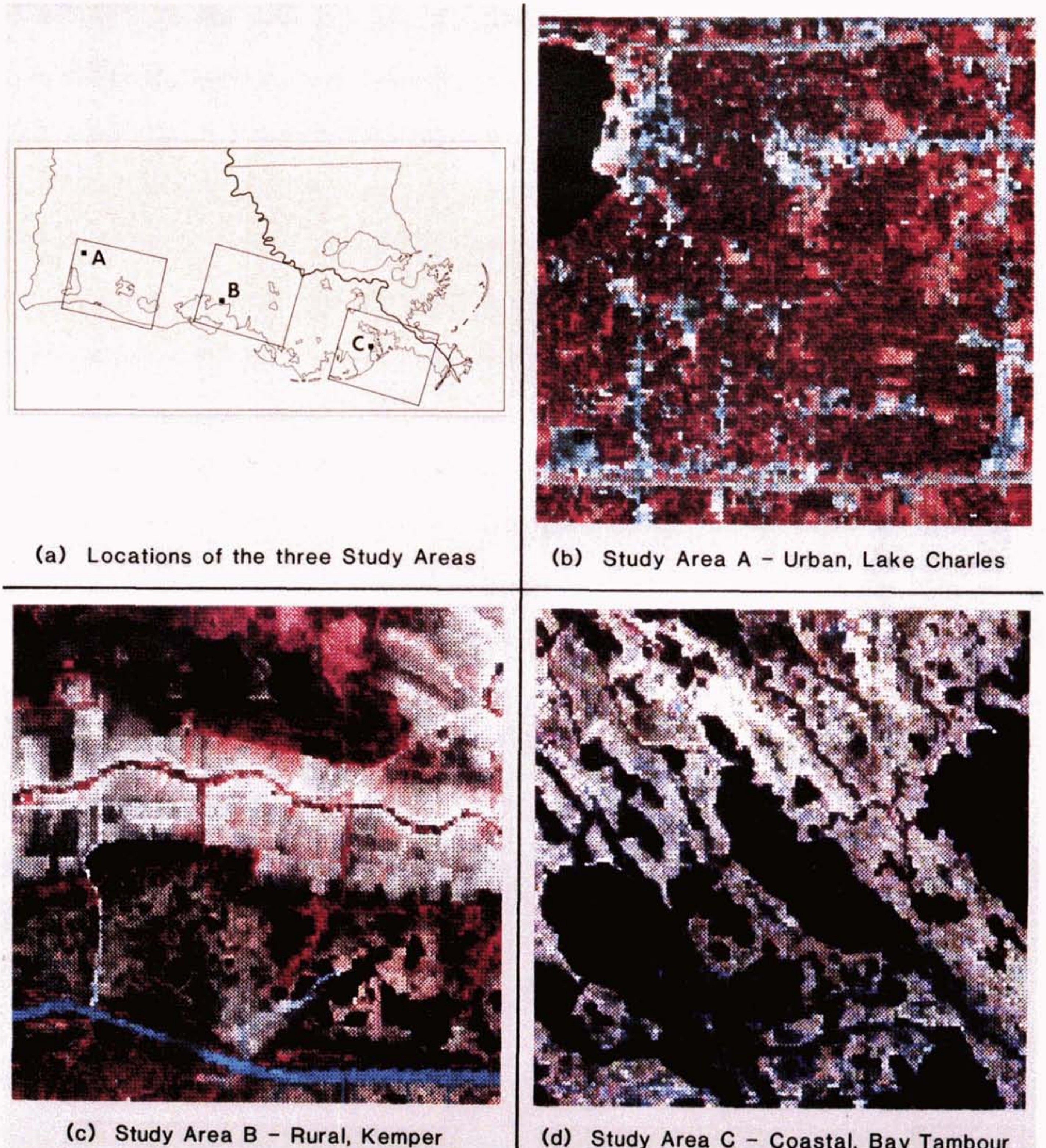

PLATE 1. Locations of the three study areas, their corresponding TM Quadrants and image displays using bands 2 (blue), 3 (green), and 4 (red). (b), (c), and (d) show study areas A (urban - Lake Charles), B (rural - Kemper), and C (coastal - Bay Tambour), respectively.

Kemper 7.5 minute quadrangle and is within St. Mary parish. It represents a rural area in coastal Louisiana characterized by scattered settlement along a major road, marsh vegetation, lakes, waterways, bayous, and pipeline channels. Study area C represents a coastal area dominated by salt-marsh vegetation, islands, and round and lagoonal lakes (Kniffen and Hilliard, 1988). The use of these three different land types provides information on how different land types respond spectrally and whether this spectral information would result in different fractal dimensions.

METHODS

Two main approaches to calculating surface dimensionality exist. The first measures the dimensionalities of the isarithmic lines (e.g., contours) characterizing the surface (Goodchild, 1980; Shelberg *et al.*, 1983), and the surface's dimension is the resultant line dimension plus one. The isarithmic lines can be digitized directly from a map or derived from the corresponding DTM surface. The second approach utilizes the variograms, either of the whole surface or of certain profiles extracted from the surface, as a basis for fractal calculation (Mark and Aronson, 1984; Roy *et al.*, 1987). This study used the isarithmic line algorithm by Shelberg *et al.* (1983), with modifications to adapt it to the VAX computer.

In brief, the algorithm operates as follows. Given a matrix of Z values, a maximum cell size (i.e., number of step sizes), and an isarithmic interval, for each isarithmic value and each cell size, the algorithm first classifies each pixel below the isarithmic value as white and that above it as black. It then compares each neighboring cell, along the rows or columns as specified by the user at the beginning, for boundary cells. The option of either using rows or columns is provided to capture any directional bias or trends that may exist along the rows or columns. The length of each isarithmic line is approximated by the number of boundary cells encountered. It is possible, for a given cell size, that no bounary cells are encountered. In this case, the isarithmic line is eliminated to avoid regression using fewer points than the given number of step sizes. This feature is especially useful to fractal calculation involving Landsat images because of the random occurrence of unusual spectral reflectance recorded at certain pixels. In effect, this feature ensures that the random "noise" in the images will not be taken into account in the calculation procedure.

After counting the number of boundary cells per cell size for each isarithmic line, a linear regression using their logarithms is performed. The D value for the surface is calculated using the following equation instead of Equation 3:

$$D = 2 - B \tag{4}$$

The surface's final fractal dimension is the average of the D values for all the isarithmic lines included.

The algorithm was applied to compute the fractal dimensions of all seven bands of the three study areas. An isarithmic interval of 2.0 and a maximum step size of 6 were used for all surfaces. In addition, both options of using rows and columns were applied to see if there are significant changes in the resultant D values. The average D values are the basis for comparison and analysis discussed in the next section. Table 2 lists the minimum, maximum, mean, and standard deviation values of each band. For ease of comparison, the coefficient of variation (standard deviation / mean) calculated for the entire study area for each band was also computed and listed, along with its average D value, in Table 2. Table 3 summarizes the D values using rows and columns, their corresponding coefficients of determination (r-squared), and the average D values. The row averages for each band and the column averages for each study area were also computed and are shown in Table 3. In addition, Figures 3a, 3b, and 3c display, in three-dimensional form, the band yielding the highest D value of each study area. These three-dimensional images serve as a useful means of comparing visually the spectral surfaces among themselves and other DTM surfaces (as shown, for example, in Figure 2). Compared with the conventional gray-scale map, the display of spectral band values in three-dimensional form has an added advantage that anomalies and groupings of values can be easily detected.

RESULTS AND DISCUSSION

The results, as summarized in Table 2, have shown that Landsat TM images generally have higher dimensions that most terrain surfaces on the Earth. This is expected because the TM data include both topographic information and non-topographic high frequencies, such as roads and edges caused by different spectral characteristics of different neighboring cover types. The spectral variability at the local scale affects the D values. With the exception of band 6, the thermal infrared band (10.4 to 12.5 μm), the resultant D values for all other bands of the three study areas range from 2.54 to 2.87, whereas most of the real-world terrain surfaces tested for other areas (using USGS 30-m DTM grid data) have dimensionalities between 2.1 and 2.5 (Shelberg *et al.*, 1983; Mark and Aronson, 1984; Roy *et al.*, 1987). The low dimension values (D = 2.16 − 2.21) for TM band 6 are partially due to the resampling procedures and partially to the original spatial resolution. Band 6 has a coarser spatial resolution of about 120 m by 120 m, compared with spatial resolutions of about 30 m by 30 m for other bands. The resampling of the original pixels into a fixed pixel size of 25 m by 25 m for all bands during the rectification process has, in effect, made the band 6 surfaces smoother, thereby resulting in lower fractal dimensions. In addition, thermal surfaces are expected to be smoother because temperature does not vary as quickly as spectral reflectance of other surface elements. An example of band 6 surface (study area **A** - Lake Charles, D=2.21) in three-dimensional form is shown in Figure 3d. This figure can be compared with Figure 3a, band 3 of the same study area (D=2.73), with the former looking much smoother.

It is interesting to note that Bay Tambour band 1 has the highest dimension (D=2.87 among all bands and study areas (Figure 3c). Yet its corresponding three-dimensional display does not look as drastic as Figures 3a or 4b, though the latter figures are of lower dimensions. This is due to the use of the same Z scale for all three-dimensional displays and because Bay Tambour band 1 has a range of Z values only between 57 and 79, the ups and downs are not shown as clearly as others which have larger Z ranges. A closer look at Figure 3c, however, indicates that it has a coarse texture with ups and downs intermingling in short distances.

An examination of the overall average D values for each band (row average in Table 3) indicates that among bands 1 to 5 and 7, band 1 generally yields the highest dimension (D=2.758), followed by bands 2, 3, 4, 7, and 5 (D=2.565). This further indicates that the spectral characteristics of neighboring cover types in a given band will affect the D values. For example, because the study areas used in this study generally have a large percentage of water, one would expect TM bands 1 and 2 to have more variability and, therefore, a larger D value than TM bands 4, 5, and 7. Among the three study areas, highest overall average dimension occurs in study area **A**, an urban area, with D=2.609 (column average in Table 3). This is followed closely by study area **C**, a complex coastal area (D=2.597). The lowest D occurs in study area **B**, a rural area, with D=2.539. The difference in these overall average D values among study areas, however, is small compared with the differences in overall Ds among bands. This implies that different land types are

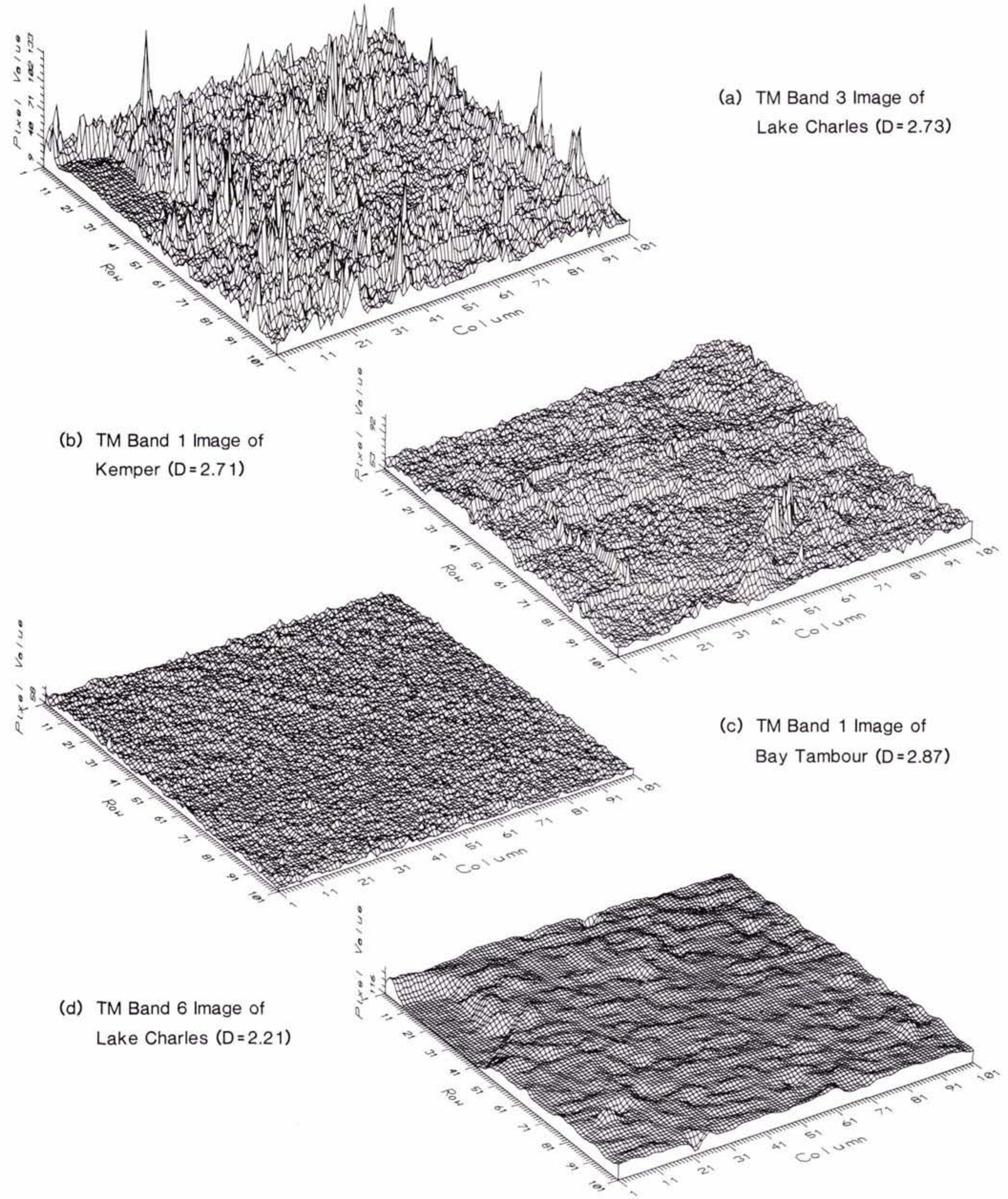

FIG. 3. Three-dimensional displays of TM surfaces. (a), (b), and (c) show the band yielding the highest *D* value of each study area. An example of band 6 surface, which is much smoother, is shown in (d).

TABLE 2. SUMMARY STATISTICS OF THE THREE STUDY AREAS

Study Area	Band	Minimum	Maximum	Mean	Standard Deviation	Coefficient of Variation	Average D
A Lake Charles	1	40	255	70.37	12.95	0.184	2.698
	2	13	126	27.40	7.57	0.276	2.715
	3	8	158	30.95	11.20	0.362	2.726
	4	4	138	45.98	11.82	0.257	2.672
	5	0	232	52.07	17.28	0.332	2.592
	6	116	146	132.37	3.61	0.027	2.208
	7	0	148	22.37	9.96	0.445	2.653
B Kemper	1	50	112	70.29	6.45	0.092	2.709
	2	13	45	26.59	4.37	0.164	2.615
	3	12	63	33.02	7.82	0.237	2.607
	4	5	70	36.10	8.43	0.234	2.587
	5	0	255	63.48	22.32	0.352	2.540
	6	94	108	99.71	2.45	0.025	2.176
	7	0	59	27.32	10.92	0.400	2.536
C Bay Tambour	1	57	79	64.08	2.05	0.032	2.866
	2	18	31	21.87	1.35	0.062	2.737
	3	15	35	22.22	3.09	0.139	2.671
	4	5	52	18.77	9.44	0.503	2.604
	5	0	56	16.44	11.70	0.712	2.562
	6	117	129	123.03	2.48	0.020	2.157
	7	0	27	8.88	5.36	0.604	2.583

TABLE 3. FRACTAL DIMENSION VALUES AND R^2 (IN BRACKETS)

	A-Lake Charles			B-Kemper			C-Bay Tambour			
Band	Row	Column	Ave. D	Row	Column	Ave. D	Row	Column	Ave. D	Row Average
1	2.635 (0.90)	2.761 (0.83)	2.698	2.689 (0.93)	2.729 (0.91)	2.709	2.859 (0.95)	2.874 (0.95)	2.866	2.758
2	2.626 (0.90)	2.805 (0.82)	2.715	2.608 (0.95)	2.623 (0.93)	2.615	2.743 (0.99)	2.731 (0.87)	2.737	2.689
3	2.631 (0.89)	2.820 (0.82)	2.726	2.586 (0.95)	2.628 (0.95)	2.607	2.697 (0.97)	2.644 (0.98)	2.671	2.668
4	2.656 (0.92)	2.687 (0.92)	2.672	2.586 (0.84)	2.588 (0.94)	2.587	2.618 (0.97)	2.591 (0.94)	2.604	2.621
5	2.596 (0.92)	2.588 (0.86)	2.592	2.476 (0.89)	2.605 (0.80)	2.540	2.577 (0.97)	2.548 (0.96)	2.562	2.565
6	2.210 (0.76)	2.206 (0.81)	2.208	2.190 (0.81)	2.161 (0.90)	2.176	2.147 (0.90)	2.167 (0.86)	2.157	2.180
7	2.650 (0.91)	2.656 (0.92)	2.653	2.513 (0.96)	2.558 (0.95)	2.536	2.550 (0.97)	2.617 (0.96)	2.583	2.591
Column Average:			2.609			2.539			2.597	

better characterized by their spectral responses to different sets of bands than by their overall average responses to all seven bands. For example, study area **A** has its highest dimensions occurring in bands 2 and 3, whereas band 1 yields the highest dimension in both study areas **B** and **C**. In other words, bands 2 and 3 of study area **A** are more spatially complex (i.e., more within-band spectral variations) and probably have higher textural information content than the other bands. These two bands may be preferred over other bands for further analysis for these particular sites for applications where texture is important. These findings could serve as a useful guideline in the future for the selection of bands for display, classificaton, and analysis.

A comparison between D values computed along rows and columns indicates that discrepancies in resultant D values are highest in study area **A** (an urban area). This is expected because directional bias is more likely to exist in urban areas where roads, highways, housing, and trees often follow certain linear patterns. As illustrated in Plate 1b, most of the roads and highways in the City of Lake Charles are aligned with rows and columns, thus resulting in greater directional bias.

The inclusion of the coefficients of variation along with the average D values in Table 2 is to illuminate the relationship between these two indices. The coefficient of variation (standard deviation / mean) of the study area is a simple aspatial statistical measure of data variability. Fractal dimension, on the other hand, can be regarded as an index of spatial complexity. As expected, there is no significant correlation between the two indices with an $r=0.32$. This result simply further asserts the need for spatial indices in analyzing spatial data that are commonly used in cartography, remote sensing, and GIS.

It should be noted that the present study has deliberately minimized the technical problems involved in the computation of fractal surface dimensionality (as discussed earlier) by applying the same maximum step size and isarithmic interval in the computation process. It is likely that, by using different maximum step sizes and isarithmic intervals, different fractal dimensions will result. The use of the same set of parameters in this study has ensured a more comparable analysis of the various TM surfaces used in this study, but not necessarily with other surfaces in other studies, because different parameters, scale ranges, and calculation methods might have been used (e.g., Mark and Aronson, 1984). Interpretations of the latter comparison therefore should be made with caution. Based on the high r-squared values in almost all of the cases (Table 3), these TM surfaces have dimensionalities between 2.54 and 2.87 at the scale range of 25m to 150m (maximum step size = 6).

Many other factors, such as striping noise, sun elevation angle, and atmospheric effect, affect the digital values of the images and thus the *D* values calculated from the images. The question of which part of the differences in *D* values is due to these noises and which part to land types remains unknown. Nevertheless, the three images used in this study were acquired at the same season (winter) and also coastal Louisiana is basically flat; therefore, the sun elevation angle effect is minimized. In addition, the fractal algorithm used here has indirectly ensured that random "noise" in the images will not be taken into account in the calculation procedure, though the effect of systematic noise, such as striping, on the *D* values has yet to be determined.

Obviously, more research is needed in order to make full and reliable use of fractals in analyzing remotely sensed data. A number of possible future studies that are directly related to the present study are suggested here. First of all, instead of comparing band-by-band or their average *D*s for different land types as in this study, one may calculate the fractal dimension of the classified image or the major component after principal component analysis and use this as basis for comparison. This may enhance compariosn among different land types. Secondly, different types of remotely sensed data other than TM images, such as MSS, SPOT, and NHAP images, should be investigated. Preferably, multiple data sets for the same study area acquired at about the same time could be acquired in order to examine the effects of various spectral and spatial resolutions on the resultant fractal dimensions. Thirdly, other spatial statistics and methods, such as spatial autocorrelation statistics, trend surface analysis, or the standard deviation of either the high pass filter or first difference/derivative image, could be applied and compared with fractal dimension. New insights could be generated on how fractals are related to these relatively well-established statistics. These research efforts will be useful to remote sensing as well as to a number of other disciplines such as spatial statistics and information science. Last but not least, the fractal dimension values derived from the present study could be used in the future as a guideline for the simulation and generation of TM images using fractal surface generation algorithms similar to the one used in generating Figure 2 (Goodchild, 1980). Additionally, different components or features in the images, which are of different scales and level of complexity, could also be generated using more complicated procedures such as the multi-fractal approach (Peitgen and Saupe, 1988), if we know beforehand the fractal dimensions of the different features in the images. The simulated TM images would be especially useful to benchmark or theoretical studies which may involve a large number of images. The use of simulated TM images could reduce not only the cost in obtaining real images, but also the possible bias existing in real images. This type of fractal application was, in fact, a major reason for measuring TM surfaces at the beginning. In addition, the simulated TM surfaces could serve as null-hypothesis images such that further analysis of normal or anomalous responses of certain land-cover types could be made.

CONCLUSIONS

The objectives of this study were to examine how different TM images and bands behave according to the fractal model and how the fractal dimensions of these TM surfaces differ from those of other surfaces. The results from the study using TM data of three different land types show that different land types have different levels of fractal dimensions in different bands. The urban area was found to be most spatially complex with high *D* values in bands 2 and 3. This is followed closely by the coastal area and the rural area, both with high *D* values in band 1. These findings may be useful in the future as guidelines for the selection of bands for subsequent display and analysis. Compared with the DTM surfaces of other areas tested in previous studies, fractal dimensions of the TM surfaces of the present three study areas are generally higher, with *D* values ranging from 2.54 to 2.87 at the scale range of 25m to 150m, as compared to values of 2.1 to 2.5 for the DTM surfaces at about the same scale range. These fractal dimension values can be used as a basis in future studies involving generation and simulation of TM images. This latter application was indeed the prime reason for its present popularity among many other disciplines. It is hoped that this study will stimulate more research in this area in the future and that this approach might provide a very different perspective in studying the various types of remotely sensed images.

ACKNOWLEDGMENTS

This research was partially supported by an LSU Council on Research Summer Grant. The author wishes to thank Bo Blackmon of the Louisiana Department of Natural Resources and Dewitt Braud of Decision Associates, Inc. for providing the original TM digital data. The staff and graduate students of the CADGIS Research Lab, in particular Farrell Jones, Hong-Lie Qiu, and David Peterson, have provided computer assistance. The staff in the Cartography Section and the Main Office of the Department of Geography and Anthropology assisted in preparing the figures and the manuscript. Comments and suggestions from anonymous reviewers are gratefully acknowledged.

REFERENCES

Arlinghaus, S. L., 1985. Fractals take a central place, *Geografiska Annaler*, Vol. 67, pp. 83–88.

Batty, M., 1985. Fractals - geometry between dimensions, *New Scientist*, Vol. 105, No. 1450, pp. 31–35.

Batty, M., and P. Longley, 1986. The fractal simulation of urban structure, *Enviornment and Planning A*, Vol. 18. pp. 1143–1179.

Barenblatt, G. I., *et al.*, 1985. The fractal dimension: A quantitative characterization of ocean-bottom relief, *Oceanology* (USSR), Vol. 24, pp. 695–697.

Bradbury, R. H., and R. E. Reichelt, 1983. Fractal dimension of a coral reef at ecological scales, *Marine Ecology Progress Series*, Vol. 10, pp. 169–171.

Burrough, P. A., 1983. Multiscale sources of spatial variation in soil. I. The application of fractal concepts to nested levels of soil variation, *Journal of Soil Science*, Vol. 34, pp. 577–597.

Carpenter, L. C., 1981. Computer rendering of fractal curves and surfaces. *Proceedings of ACM SIGGRAPH Conference*, Seattle, Washington, July, 1980.

Clark, N. N., 1986. Three techniques for implementing digital fractal analysis of particle shape, *Powder Technology*, Vol. 46, pp. 45–52.

De Cola, L., 1987. Fractal analysis of digital landscapes simulated by two spatial processes. Paper presented at the Annual Meeting of the Association of American Geographers, Portland.

Dutton, G. H., 1981. Fractal enhancement of cartographic line detail, *The American Cartographer*, Vol. 8, pp. 23–40.

Feder, J., 1988. *Fractals*, Plenum Press, New York, New York.

Fournier, A., D. Fussell, and L. C. Carpenter, 1982. Computer rendering of stochastic models, *Communications, Association for Computing Machinery*, Vol. 25, pp 371–384.

Goodchild, M. F., 1980. Fractals and the accuracy of geographical measures, *Mathematical Geology*, Vol. 12, pp. 85–98.

Goodchild, M. F., and D. M. Mark, 1987. The fractal nature of geographic phenomena, *Annals of the Association of American Geographers*, Vol. 77, No. 2, pp. 265–278.

Hakanson, L., 1978. The length of closed geomorphic lines, *Mathematical Geology*, Vol. 10, pp. 141–67.

Jiang, R-S., 1984. *An Evaluation of Three Curve Generation Methods*, M. S. Thesis, Department of Geography, The Ohio State University, Columbus, Ohio.

Kniffen, F. B., and S. B. Hilliard, 1988. *Louisiana - Its Land and People*, Revised Edition, Louisiana State University Press, Baton Rouge, Louisiana, 213 p.

Lam, N. S-N., 1982. An evaluation of areal interpolation methods, *Proceedings, Fifth International Symposium on Computer-Assisted Cartography (Auto-Carto 5)*, Vol. 2, pp. 471–79.

———, 1983. Spatial interpolation methods: A review, *The American Cartographer* Vol. 10, pp. 129–49.

Loehle, C., 1983. The fractal dimension and ecology, *Speculations in Science and Technology*, Vol. 6, No. 2, pp. 131–142.

Lovejoy, S., and B. B. Mandelbrot, 1985. Fractal properties of rain, and a fractal model, *Tellus*, Vol. 37A, pp. 209–232.

Mandelbrot, B. B., 1967. How long is the coast of Britain? Statistical self-similarity and fractional dimension. *Science*, Vol. 156, pp. 636–638.

———, 1977. *Fractals: Form, Chance and Dimension*, Freeman, San Francisco, California.

———, 1983. *The Fractal Geometry of Nature*, Freeman, San Francisco, California.

Mark, D. M., 1984. Fractal dimension of a coral reef at ecological scales: A discussion, *Marine Ecology Progress Series*, Vol. 14, pp. 293–94.

Mark, D. M., and P. B. Aronson, 1984. Scale-dependent fractal dimensions of topographic surfaces: An empirical investigation, with applications in germorphology and computer mapping, *Mathematical Geology*, Vol. 11, pp. 671–684.

Mark, D. M., and J. P. Lauzon, 1984. Linear quadtrees for geographic information systems, *Proceedings, International Symposium on Spatial Data Handling*, Zurich, Switzerland, pp. 412–430.

Obrach, R., 1986. Dynamics of fractal networks, *Science*, Vol. 231, pp. 814–819.

Peitgen, H.-O., and P. H. Richter, 1986. *The Beauty of Fractals*, Springer-Verlag, New York.

Peitgen, H.-O., and D. Saupe, 1988. *The Science of Fractal Images*, Springer-Verlag, New York.

Phillips, J. D., 1986. Spatial analysis of shoreline erosion, Delaware Bay, New Jersey, *Annals of the Association of American Geographers*, Vol. 76, No. 1, pp. 50–62.

Richardson, L. F., 1961. The problem of contiguity, *General Systems Yearbook*, Vol. 6, pp. 139–187.

Rothrock, D. A., and A. S. Thorndike, 1980. Geometric properties of the underside of sea ice, *Journal of Geophysical Research*, Vol. 85, No. C7, pp. 3955–3963.

Roy, A. G., G. Gravel and C. Gauthier, 1987. Measuring the dimension of surfaces: A review and appraisal of different methods, *Proceedings, Eight International Symposium on Computer-Assisted Cartography (Auto-Carto 8)*, Baltimore, pp. 68–77.

Shelberg, M. C., H. Moellering, and N. S-N. Lam, 1982. Measuring the fractal dimensions of empirical cartographic curves. *Proceedings, Fifth International Symposium on Computer-Assisted Cartography (Auto-Carto 5)*, Washington, D.C., pp. 481–490.

Shelberg, M. C., N. S-N. Lam, and H. Moellering, 1983. Measuring the fractal dimensions of surfaces. *Proceedings, Sixth International Symposium on Automated Cartography (Auto-Carto 6)*, Ottawa, Ontario, Canada, Vol. 2, pp. 319–328.

(Received 14 September 1988; revised and accepted 10 March 1989)